

Background Level of Atmospheric Radon-222 Concentrations at Gosan Station, Jeju Island, Korea in 2011

Won-Hyung Kim, Hee-Jung Ko, Chul-Goo Hu,[†] Haeyoung Lee,[‡] Chulkyu Lee,[‡]
S. Chambers,[§] A. G. Williams,[§] and Chang-Hee Kang^{*}

*Department of Chemistry, Jeju National University, Jeju 690-756, Korea. *E-mail: changhee@jejunu.ac.kr*

[†]Department of Environmental Engineering, Jeju National University, Jeju 690-756, Korea

[‡]Korea Global Atmosphere Watch Center, Korea Meteorological Administration, Chungnam 357-961, Korea

[§]Australian Nuclear Science and Technology Organisation, Locked Bag 2001, Kirrawee DC, NSW 2232, Australia

Received December 16, 2013, Accepted December 27, 2013

Real-time monitoring of hourly atmospheric radon (Rn-222) concentration was performed throughout 2011 at Gosan station, Jeju Island, one of the least polluted regions in Korea, in order to characterize the background levels, and temporal variations on diurnal to seasonal time-scales. The annual mean radon concentration for 2011 was 2527 ± 1356 mBq m⁻³, and the seasonal cycle was characterized by a broad winter maximum, and narrow summer minimum. Mean monthly radon concentrations, in descending order of magnitude, were Oct > Sep > Feb > Nov > Jan > Dec > Mar > Aug > Apr > Jun > May > Jul. The maximum monthly mean value (3595 mBq m⁻³, October), exceeded the minimum value (1243 mBq m⁻³, July), by almost a factor of three. Diurnal composite hourly concentrations increased throughout the night to reach their maximum (2956 mBq m⁻³) at around 7 a.m., after which they decreased to their minimum value (2259 mBq m⁻³) at around 3 p.m. Back trajectory analyses indicated that the highest radon events typically exhibited long-term continental fetch over Asia before arriving at Jeju. In contrast, low radon events were generally correlated with air mass fetch over the North Pacific Ocean. Radon concentrations typical of predominantly continental, and predominantly oceanic fetch, differed by a factor of 3.8.

Key Words : Radon-222, Atmospheric radon, Background level, Gosan Station, Back trajectory

Introduction

Naturally occurring radionuclides (*e.g.* ⁷Be, ¹⁰Be, ²¹⁰Pb, and ²²²Rn) and anthropogenic radionuclides (*e.g.* ⁸⁵Kr) are important isotopes for studying atmospheric processes. As such, their continuous monitoring is encouraged, and considered an essential component of WMO/GAW (World Meteorological Organization/Global Atmospheric Watch air quality observations).¹⁻³ Radon-222 (radon), in particular, is an inert gas resulting from the alpha decay of radium in the uranium-238 decay chain. It has a half-life of 3.82 days, and is released into the atmosphere from most rock and soil types. In conjunction with other radionuclide measurements, such as ²¹⁰Pb, radon data provides a useful constraint for the evaluation of air transport models and identifying global atmospheric conditions. Because terrestrial radon fluxes are typically 2-3 orders of magnitude greater than oceanic fluxes, it is useful as a tracer for air masses which have recently passed over land. The large radon concentration difference between terrestrial and oceanic fetch regions can be used to indicate whether recent (2-3 week) air mass fetch history has been primarily over continents or the ocean. Radon is also an excellent tracer for studying vertical mixing and transport of greenhouse gases. Data collected at GAW monitoring stations is essential for the advancement of our understanding of the relationship between long-term changes in atmospheric composition and changes in global and regional climate, as well

as the long-range atmospheric transport and deposition of potentially harmful substances over a range of ecosystems.⁴

Furthermore, radon accounts for 50% of the public's exposure to naturally-occurring sources of radiation. In many countries, radon is the second most important cause of lung cancer after smoking. The proportion of lung cancers attributable to radon is estimated to range from 3 to 14%.⁵ To improve our understanding, and assist in the management of natural radioactive substances in atmosphere, it is essential to monitor radon concentrations under a wide range of atmospheric conditions, and to characterise seasonally varying outdoor background concentrations in clean-air regions as a reference point for other indoor and outdoor investigations. Since radon is a passive atmospheric tracer with a single source (land) and single sink (radioactive decay), it is a convenient means of estimating the degree of air mass contact with terrestrial based pollutant sources, as well as atmospheric mixing/dilution. For these reasons, co-located continuous observations of radon and various atmospheric pollutants at key locations should be encouraged because an understanding of atmospheric concentration/dilution effects on precursor species advected to the Korean Peninsula from Asia on the prevailing westerlies is a critical prerequisite to accurately predicting the formation of secondary pollution products that have potentially adverse health effects.

Jeju Island is one of the cleanest regions in Korea, contributing comparatively little to regional air pollution.⁶ It is

well situated, however, to observe the outflow of natural and anthropogenic atmospheric pollutants from the East Asian region. Consequently, Jeju Island – and Gosan station in particular – has been the focal point of several major initiatives pertaining to regional air quality and understanding the climatic effects of aerosols, including PEM (Pacific Exploratory Mission)-West A, PEM-West B, ACE (Aerosol Characterization Experiment)-Asia and ABC (Atmospheric Brown Cloud) projects.⁷⁻⁹ Gosan station, maintained by the Korean Meteorological Administration, is located on the western extremity of Jeju Island on the grounds of the Jeju upper air meteorological station. It is a long-term monitoring facility for various air quality parameters and atmospheric radon.

Indoor and underground spaces, where high levels of radon can accumulate due to restricted ventilation, are the main subject of radon monitoring and control strategies in Korea. However, until now, reference monitoring for such studies in the ambient atmosphere has rarely been performed. While the Gosan Station air quality monitoring program has been in operation since the early 1990s, continuous hourly radon monitoring began almost a decade later.¹⁰ The purpose of this study is to provide an overview and background levels of atmospheric radon in Korea from its real-time monitoring at Gosan station in Jeju Island.

Experimental

Location and Site Characteristics. Jeju Island is located about 100 km south of the Korean Peninsula, about 500 km west of China (Jiangsu province), and about 200 km east of the Japanese Islands (Kyushu), as shown in Figure 1. Due to its comparatively low population density and limited industry, Jeju Island has few local emissions of air pollutants and is one of the cleanest areas in Korea. Consequently it is an excellent location to study the transport and transformation of ambient trace species in the northeast Asia region, and to study the impact of continental outflow. Gosan station is on

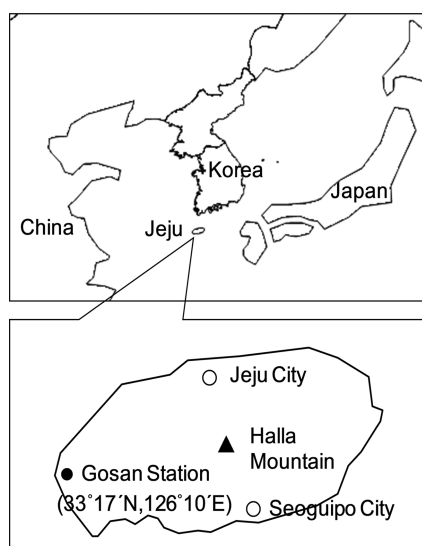


Figure 1. Location of Gosan Station on Jeju Island, Korea.

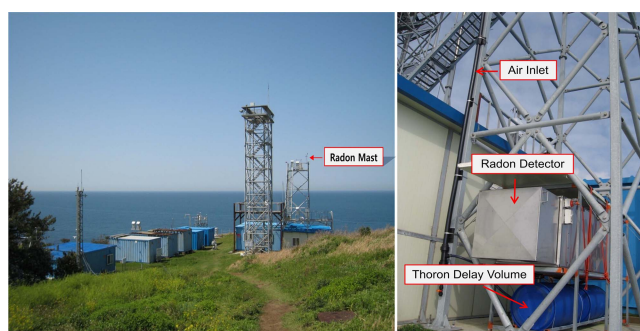


Figure 2. Installation of the 1500 L radon detector (D1500) and 400 L thoron delay volume, at the base of the 10 m scaffold tower at Gosan station on Jeju Island.

the western extremity of Jeju Island, situated 10 m from the edge of a sheer bluff that rises approximately 72 m above sea level.^{7,11}

Atmospheric Radon Measurement. Continuous, hourly atmospheric radon measurements were made at Gosan station from January to December 2011 using a 1500 L dual flow loop, two filter radon detectors (Figure 2) designed and built at the Australian Nuclear Science and Technology Organisation (ANSTO). This kind of detector provides a direct measurement of the ambient atmospheric radon concentration that is independent of the concentration of radon progeny in the atmosphere, or the level of equilibrium established between radon and its progeny.^{10,12,13}

The detector sampled air at approximately 50 L min⁻¹ through a 50 mm HDPE intake line from a height of approximately 10 m agl. The detector's response time was around 45 minutes, and at the time of commissioning the lower limit of detection was approximately 30 mBq m⁻³. Typically the detector was calibrated on a monthly basis by injecting radon for 5 hours from a Pylon 18.5 ± 4% kBq Ra-226 source traceable to NIST standards. The instrumental background, which varies primarily as a function of ²¹⁰Pb (half-life 22.3 y) loading on the detector's second filter, was characterised every 3 months.

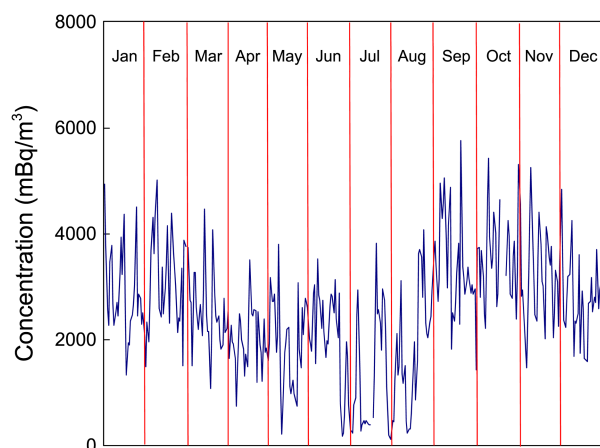
The raw radon counts and all detector diagnostic parameters are recorded every 30 minutes using a Campbell Scientific data logger (CR800), and then transferred by serial link to the nearby controlling computer, and the half hourly data is aggregated to hourly values after calibration and quality checks. All times used throughout this study are local standard time (UTC +9h).

Results and Discussion

Background Radon-222 Concentrations. The ambient background level of atmospheric radon in Korea throughout 2011 was measured using a real-time monitoring system at Gosan station, and the results are shown in Table 1 and Figure 3. Over the study period the mean annual radon concentration was 2527 mBq m⁻³. By comparison, averages of monthly 90th and 10th percentiles over this year were 5175 mBq m⁻³ (n = 839) and 361 mBq m⁻³ (n = 839), respective-

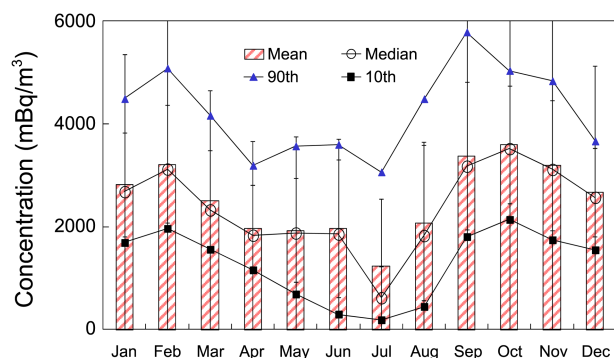
Table 1. Atmospheric radon concentrations at Gosan and other sites

Site	Concentration (mBq m ⁻³)	Periods
Seoul, Korea ¹⁵	7620 ± 4110	1999. 12-2002. 1
Sado Island, Japan ¹⁴	2555 ± 261	2002-2004
Hok Tsui, Hong Kong ¹⁴	5580 ± 626	2002-2004
Mauna Loa, Hawaii ¹⁶	102	2004-2010
Hong Kong ¹⁷	9300	2007. 11-2008. 10
Milan, Italy ¹⁸	9500	2000
This Study	2527 ± 1356	2011. 1-12

**Figure 3.** Yearly time series variation of daily radon concentration measured at Gosan station in 2011.

ly, showing about a factor of 14 difference. The seasonal cycle indicated by the monthly mean and 90th percentile concentrations was similar (Figure 4), but that of the 10th percentile values - less affected by atmospheric stagnation events in May/June - showed a slightly different pattern in spring. The mean radon concentration at Seoul (7620 mBq m⁻³) over the same period was about 3.0 times higher than at Gosan (Table 1). Compared to other foreign regions, the Gosan radon concentration was 2.2 times lower than at Hok Tsui, Hong Kong, but 24.8 times higher than at Mauna Loa, Hawaii. Especially, the radon concentration at Gosan was almost 3.7 times lower than at King's Park Meteorological Station in Hong Kong, and Milan, a metropolis of Italy, showing the characteristic of a background area.^{10,14}

Monthly Variation of Radon-222 Concentration. Daily mean Gosan radon observations (Figure 3) show a pronounced seasonality characterized by high concentrations in winter and low concentrations in summer. During the winter monsoon, air flow in the lower atmosphere is directed from the Asian continent toward the Pacific; the converse is true in summer. In this study, high radon concentrations (2666-3595 mBq m⁻³) were observed from September to February (Figure 4). This is the period of most consistent terrestrial fetch due to strong northerly to north westerly wind component and drier air masses, during the height of the Asian winter monsoon. For the most part, mean monthly wind

**Figure 4.** Distributions (10th/50th/90th percentiles) of mean monthly radon concentrations at Gosan station.

speeds are high between December and March when air masses more frequently sweep down from Mongolia/Siberia.¹⁹

The lowest mean monthly radon concentrations (1243 mBq m⁻³) were observed in July, which was a period of relatively dominant oceanic fetch owing to strong southerly component of wind direction and humid air masses. As previously outlined, the ocean is a negligible source of radon. Based on mean monthly relative humidity values, the most consistent oceanic fetch occur at the height of the summer monsoon, consistent with southerly mean monthly wind directions for June-August. A narrow window, of only 2-3 weeks in July and August, of very low radon concentrations was observed (Figure 3), associated with the least terrestrially perturbed Pacific Ocean air masses that arrive from the south, around the western Pacific anticyclone.

Diurnal Variation of Radon-222 Concentration. As well as the monthly variability in radon concentrations described above, there was a pronounced diurnal variability at Gosan site. Since the radon source function of a given fetch region usually changes little with time, most of the variability in radon concentration observed at Gosan on sub-diurnal time-scales is due to the dilution of locally emitted radon within the atmospheric boundary layer (ABL). However, this is not the case for all sites. Studies at the Mauna Loa Observatory in Hawaii have identified a diurnal cycle characterized by an early afternoon maximum and mid-morning minimum. The diurnal cycle at this high-elevation, mountain site, can be primarily attributed to anabatic/Katabatic flows that bring radon from the island and volcano flanks to the observatory. The longest land fetch (across the island and up the mountain) occurs for the anabatic flow conditions, resulting in the early afternoon maximum values. Minimum concentrations, most representative of tropospheric air between 3.3-4.1 km, are seen mid-morning, in the lull period between anabatic and katabatic flow conditions.¹⁶ The diurnal cycle of radon at Gosan, however, was considerably different. The 2011 diurnal composite radon cycle at Gosan was characterized by an early morning minimum (7 a.m.) and mid-afternoon minimum (3 p.m.). This cycle had an amplitude of 697 mBq m⁻³; larger than that at Mauna Loa, but smaller than typically observed at a continental site. The highest nocturnal composite concentrations (2956 mBq m⁻³)

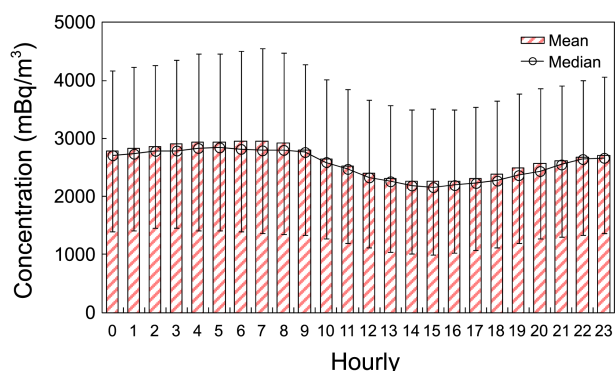


Figure 5. Diurnal variation of hourly mean radon concentrations at Gosan station.

were observed around sunrise when atmospheric mixing depths were shallowest, and the lowest values (2259 mBq m^{-3}) in the early afternoon when mixing depths were greatest (Figure 5).

In winter, air mass fetch to Gosan is mostly across the Yellow Sea. Since significant water bodies have a large heat capacity, they exhibit small diurnal changes in surface temperature. Consequently, large water bodies have a stabilizing effect on the atmospheric mixing depth, resulting in comparatively little diurnal variability in mixing depth (atmospheric dilution) at Gosan in winter (Figure 6). This is reflected in the small amplitude of the composite diurnal radon cycle at the site compared to that typical of inland sites. Conversely, in summer, most of the air mass fetch to Gosan is across Jeju Island (a land fetch of around 70 km), resulting in a much larger diurnal variation in atmospheric mixing depth due to the comparatively large diurnal change in surface temperature, more typical of continental sites.²⁰ The corresponding amplitude of the summertime composite diurnal radon concentration at Gosan is large.

Fetch Effects of Radon-222 Concentrations. To examine the influence of air mass pathways on the variability of atmospheric radon concentrations at Gosan, a back trajectory analysis was carried out. 5-Day trajectories were computed using the HYSPLIT (HYbrid Single-Particle Lagrangian Integrated Trajectory) model developed by NOAA/ARL (National Oceanic and Atmospheric Administration/Air Re-

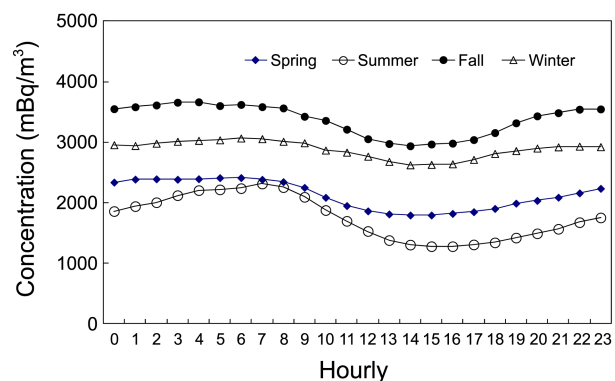


Figure 6. Diurnal pattern of hourly radon concentration for four seasons at Gosan.

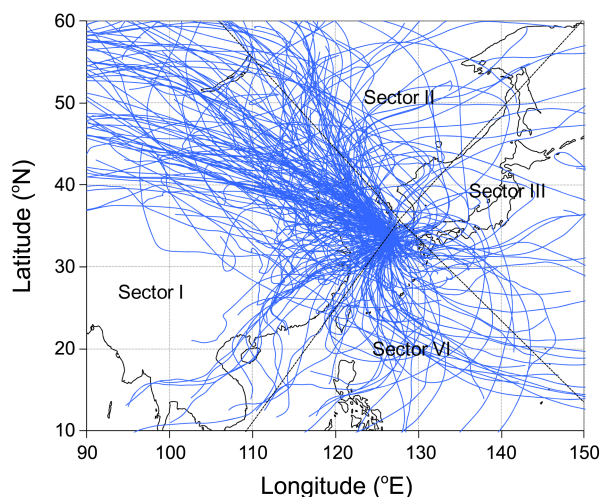


Figure 7. Sectional classification of back trajectory analysis by 4 pathway types for air mass transport; Sector I: China continent, Sector II: Korea peninsular/Russia, Sector III: Japan/East Sea, Sector IV: North Pacific Ocean.

Table 2. Sectional radon concentrations in accordance with 4 pathway types for air mass transport

Statistics	Concentration (mBq m^{-3})			
	Sector I (n=286)	Sector II (n=7)	Sector III (n=29)	Sector IV (n=37)
Mean	2751.4	2528.7	2671.8	722.3
S.D.	942.9	656.5	1158.9	686.5

sources Laboratory).²¹

In conjunction with radon observations, back trajectory analyses were used to identify specific regions within four main fetch categories that are most represented by the reported air quality statistics. For the study, back trajectory analyses were grouped in the following four fetch categories (Figure 7): (1) Sector I: China continent; (2) Sector II: Korea Peninsular/Russia; (3) Sector III: Japan/East Sea; and (4) Sector IV: North Pacific Ocean. A comparison was made between the mean radon concentrations in each sector (Table 2). Mean concentrations for Sector I, II, III, and IV were 2751.4 , 2528.7 , 2671.8 , and 722.3 mBq m^{-3} , respectively. Sources of radon are primarily terrestrial, with corresponding fluxes from open bodies of water being 2-3 orders of magnitude lower.^{20,22} In this study, the radon concentration in air masses moving from China (Sector I) was about 3.8 times higher than that from the North Pacific Ocean (Sector IV).

Conclusions

Real-time, continuous hourly observations of atmospheric radon concentration at Gosan station were used to characterize temporal variability on diurnal to seasonal timescales and investigate predominant air mass fetch pathways. The annual mean radon concentration in 2011 was 2965 mBq m^{-3} , with a seasonal variability characterized by high values in

winter and low values in summer. The highest radon concentrations – usually within the range of 2666-3595 mBq m⁻³ – were typically observed from September to February, when strong northerly winds and extended terrestrial fetch were common. The lowest mean monthly radon concentration (1243 mBq m⁻³) was observed in July, a period of southerly wind direction and relatively dominant oceanic air mass fetch. The diurnal composite radon concentration at Gosan had an amplitude of 697 mBq m⁻³ was characterized by an early morning (7 a.m.) maximum (2956 mBq m⁻³) and a mid-afternoon (3 p.m.) minimum (2259 mBq m⁻³). Based on air mass back trajectory analyses, the radon concentration of air mass with a recent fetch over China were larger than those of air masses with recent fetch predominantly over the North Pacific Ocean, by a factor of 3.8.

Acknowledgments. This work was funded by the Korea Meteorological Administration Research and Development Program under Grant CATER 2012-3010.

References

1. WMO/GAW, *Global Atmosphere Watch Measurements Guide (No. 143)*; WMO TD No. 1073, July 2001; p 55.
2. Zhang, K.; Feichter, J.; Kazil, J.; Wan, H.; Zhuo, W.; Griffiths, A. D.; Sartorius, H.; Zahorowski, W.; Ramonet, M.; Schmidt, M.; Yver, C.; Neubert, R. E. M.; Brunke, E.-G. *Atmos. Chem. Phys.* **2011**, *11*, 7817.
3. IAEA/WMO, *Sources and Measurements of Radon and Radon Progeny Applied to Climate and Air Quality Studies: IAEA Proceeding Series*, International Atomic Energy Agency Vienna International Centre, 2012; pp 9-14.
4. Zahorowski, W.; Chambers, S. D.; Henderson-Sellers, A. *J. Environ. Radioact.* **2004**, *76*, 3.
5. WHO, *Radon and cancer*, WHO Media centre, 2009 (<http://www.who.int/mediacentre/factsheets/fs291/en/>).
6. Kim, Y. P.; Shim, S.-G.; Moon, K. C. *J. Appl. Meteorol.* **1998**, *37*, 1117.
7. Park, M. H.; Kim, Y. P.; Kang, C.-H.; Shim, S.-G. *J. Geophys. Res.* **2004**, *109*(D19S13), doi:10.1029/2003JD004110.
8. Huebert, B. J.; Bates, T.; Russell, P. B.; Shi, G.; Kim, Y. J.; Kawamura, K.; Carmichael, G.; Nakajima, T. *J. Geophys. Res.* **2003**, *108*(D23), 8633, doi:10.1029/2003JD003550.
9. Nakajima, T.; Yoon, S. C.; Ramanathan, V.; Shi, G. Y.; Takemura, T.; Higurashi, A.; Takamura, T.; Aoki, K.; Sohn, B. J.; Kim, S. W.; Tsuruta, H.; Sugimoto, N.; Shimizu, A.; Tanimoto, H.; Sawa, Y.; Lin, N. H.; Lee, C. T.; Goto, D.; Schutgens, N. *J. Geophys. Res.* **2007**, *112*(D24S91), doi:10.1029/2007JD009009..
10. Zahorowski, W.; Chambers, S.; Wang, T.; Kang, C. H.; Uno, I.; Poon, S.; Oh, S. N.; Werczynski, S.; Kim, J.; Henderson-Sellers, A. *Tellus* **2005**, *57*(2), 124.
11. Kim, N. K.; Kima, Y. P.; Kang, C. H. *Atmos. Environ.* **2011**, *45*(34), 6107.
12. Whittlestone, S.; Zahorowski, W. *J. Geophys. Res.* **1998**, *103*(D13), 16,743.
13. Chambers, S.; Williams, A. G.; Zahorowski, W.; Griffiths, A.; Crawford, J. *Tellus* **2011**, *63B*, 843.
14. Chambers, S.; Zahorowski, W.; Matsumoto, K.; Uematsu, M. *Atmos. Environ.* **2009**, *43*(2), 271.
15. Kim, Y. S.; Lee, C. M.; Kim, K. Y.; Jeon, H. J.; Kim, J. C.; Iida, T. *Kor. J. Env. Hlth.* **2007**, *33*(4), 283.
16. Chambers, S. D.; Zahorowski, W.; Williams, A. G.; Crawford, J.; Griffiths, A. D. *J. Geophys. Res.* **118**, 1-13, doi:10.1029/2012JD018212.
17. Chan, S. W.; Lee, C. W.; Tsui, K. C. *J. Environ. Radioact.* **2010**, *101*(6), 494.
18. Sesana, L.; Caprioli, E.; Marazzan, G. M. *J. Environ. Radioact.* **2003**, *65*(2), 147.
19. Guttikunda, S. K.; Thongboonchoo, N.; Arndt, R. I.; Calori, G.; Carmichael, G. R.; Streets, D. G. *Water, Air, and Soil Pollution*, **2001**, *131*, 383.
20. Williams, A. G.; Chambers, S. D.; Zahorowski, W.; Crawford, J.; Matsumoto, K.; Uematsu, M. *Tellus* **2009**, *61B*, 732.
21. Draxler, R. R.; Rolph, G. D. *HYSPLIT (HYbrid Single-Particle Lagrangian Integrated Trajectory) Model access via NOAA ARL READY Website*, 2013 (http://ready.arl.noaa.gov/HYSPLIT_traj.php).
22. Zhuo, W.; Guo, Q.; Chen, B.; Cheng, G. *J. Environ. Radioact.* **2008**, *99*, 1143.